

# Report on the proof-of-concept evaluation of SOPs for innovative *in vitro* models and mechanistically relevant assays for nanosafety human hazard assessment

## DELIVERABLE 5.4

**Due date of Deliverable:** M46  
**Actual Submission Date:** 31.10.2022  
**Responsible partner:** SU, Wales, UK  
**Report Author(s):** Michael J Burgum, Shareen H Doak, Martin JD Clift  
**Reviewed by:** WP5 Partners; Maria Dusinska, Eleonora Longhin (NILU, PMO)  
**Nature:** Document, report  
**Dissemination Level:** PU = Public

**Call:** H2020-NMBP-13-2018  
**Topic:** Risk Governance of nanotechnology  
**Project Type:** Research & Innovation Action (RIA)  
**Name of Lead Beneficiary:** NILU, Norway  
**Project Start Date:** 1 January 2019  
**Project Duration:** 50-Months



## Document History

<i>Version</i>	<i>Date</i>	<i>Authors/ who acted</i>	<i>Comment</i>	<i>Modifications made by</i>
<i>0.1</i>	18.11.2021	Michael J Burgum (SU)	First Draft	Prof. Shareen H Doak (SU)
<i>0.2</i>	21.08.2022	Michael J Burgum (SU)	Additions made for Month 46 submission	Prof. Shareen H Doak (SU)
<i>0.3</i>	25.09.2022	Elisa Moschini (LIST)	Lung data and results/discussion	Michael J Burgum
<i>0.4</i>	27.09.22	Prof. Shareen H Doak	Additions	Prof. Shareen H Doak
<i>0.5</i>	30.09.22	Eleonora Longhin, Naouale El Yamani (NILU)	Additions	Michael J Burgum
<i>0.6</i>	12.10.22	Valerie Fessard	Addition of all HepaRG data and results, conclusions	Michael J Burgum
<i>1.0</i>	31.10.2022	PMO (NILU)	Submitted to the EC	Eleonora Longhin, Maria Dusinska



## Abstract

Task 5.3 led by SU has been focused on the evaluation of advanced *in vitro* models, as compared to standard *in vitro* and *in vivo* hazard characterisation systems for engineered nanomaterials (ENMs). The aim of this task was to compare the ability of these advanced model systems cultured either in three dimensional (3D) or consisting of multiple cell types to report on a variety of hazard endpoints when exposed to ENMs. Their performance has been compared to the equivalent outputs from less complex, yet well-established 2D monoculture systems. This allowed us to determine if the innovative advanced models are more-, or less-predictive of ENM-induced damage than monocultures.

To achieve these goals each partner contributing to this task performed extensive literature searching using online databases to first gather all the relevant literature pertaining to each tissue being modelled e.g., the liver or lung. This process was followed for advanced *in vitro* models, well-established 2D *in vitro* models and finally a comparison was made against *in vivo* models. To ensure high quality data was being collected and archived in the spreadsheets each partner implemented an agreed-upon quality control measure on each publication, referred to as the GUIDEnano quality criteria. This method of critically appraising the scientific quality of each paper was first published in 2018 and was implemented on this task and subsequently on other tasks. The data generated by this quality control measure has been collated into a final format based on each partners individual efforts.

Once all three model-types had been gathered, partners then performed comparisons; advanced *in vitro* vs. *in vivo*, and advanced *in vitro* vs. 2D *in vitro* monoculture models cross-referencing against specific ENMs and biological endpoints such as cytotoxicity for example. This level of analysis allowed us to narrow down the tissues to explore in the experimental work and highlight several key models from the literature. From this analysis we determined the most promising systems to take forward for a small inter-laboratory trial were the 3D spheroid liver model developed in the PATROLS project and a lung tetra-culture model developed at LIST. The purpose of this interlaboratory trial was to determine if reproducible data could be achieved using known standard operating protocols (SOPs) for each of these methods, using ENMs and concentrations utilised in Task 5.1.



**Contents**

Document History ..... 2

Abstract..... 3

Introduction..... 5

Critical Literature Review ..... 8

    Results of inter-laboratory experimental work ..... 24

Advanced Liver Model Data ..... 25

Advanced Lung Models ..... 27

VitroCell Deposition curves at SU ..... 28

VitroCell Exposure Deposition ..... 29

Endpoint data ..... 29

ENM-assay interference-check at LIST ..... 30

    Experimental work on HepaRG cells conducted at ANSES..... 31

Advanced 3D HepaRG liver model ..... 31

2D HepaRG model ..... 35

ENM-assay interference-check at ANSES ..... 39

    Conclusions..... 42

Advanced Liver Models ..... 42

Endpoint data ..... 42

Advanced Lung Models ..... 42

VitroCell Deposition ..... 42

Endpoint data..... 43

HepaRG Data ..... 43



## List of Abbreviations

3D - 3-dimensional

AB - Alamar Blue solution

ANSES - Administración Nacional de la Seguridad Social, RiskGONE's partner

ELISA - Enzyme-linked immunosorbent assay

ENM - engineered nanomaterial

Fpg - Formamidopyrimidine-DNA Glycosylase

GI - gastrointestinal

IMI - Institute for Medical Research and Occupational Health, RiskGONE's partner

KU Leuven - Katholieke Universiteit Leuven, RiskGONE's partner

LDH - lactate dehydrogenase

LIST – Luxembourg Institute of Science and Technology, RiskGONE's partner

LPS - lipopolysaccharide

MMS - methyl methanesulfonate

MTT - 3-[4,5-dimethylthiazol-2-yl]-2,5 diphenyl tetrazolium bromide

NILU - Norwegian Institute for Air Research, RiskGONE's coordinator and partner

SEM - standard error of the mean

SOPs - standard operating procedures

SU - Swansea University, RiskGONE's partner

TBE - Trypan blue exclusion

TEM – transmission electron microscopy

UiB - Universitetet i Bergen



## Introduction

Past FP7, EURONANOMED, Horizon 2020 and other international projects (e.g., PATROLS, npSCOPE, NANoREG, NANoREG2, HISENTS, caLIBRAte, NanoTEST, GEMNS, INNOCENT, etc.) were aimed towards developing state-of-the-art *in vitro* models which more closely mimic human architecture. Examples being advanced *in vitro*, 3-dimensional (3D) models of the lung, liver, brain, gastrointestinal (GI) tract, lab-on-a-chip, and microfluidic systems. These projects were also developing Adverse Outcome Pathways (AOPs) to ensure interference-free, mechanistically relevant biological endpoint testing, for example in, cytotoxicity, genotoxicity, oxidative stress, immune response, omics, and DNA sequencing assays.

Task 5.3 of RiskGONE has evaluated the data available (in the literature, predominantly) for a range of advanced test systems representing key human organs of engineered nanomaterial (ENM) exposure and included in this review a critical analysis with robust quality screening processes to support our decision making for the final experimental testing. The literature data pertaining to each of the relevant tissues being modelled was collected by first investigating the human hazard posed by ENMs in the advanced, 3D *in vitro* models, followed by the less advanced 2D *in vitro* test systems (available from projects such as NANoREG, NANoREG2, caLIBRAte) and finally *in vivo* models. Following this methodology, a catalogue of the most robust models in each category was generated with supporting quality criteria for each publication covering ENM physico-chemical characterisation and biological test system characterisation.

Subsequently, the research outputs from the advanced *in vitro* models were directly compared to those of the *in vitro* monoculture models and the *in vivo* models, cross referencing by the test ENM used and biological endpoints allowing for direct read-across comparisons. In these comparisons it could be determined whether the research outputs from the advanced models were more- or less-predictive of ENM toxicity than standard assays and how close they come to mimicking biological responses observed in physiologically comparable *in vivo* models, except for some advanced models that are certainly relevant but with unfortunately not enough dataset for elaborating a comparison (HepaRG cells).



From the comparisons performed by each contributing partner and the final conclusions drawn, the most optimal models sourced from the literature and supported by the research expertise of contributing partners, one model was selected for the lung and liver respectively. The advanced model for the lung was the 3D alveolar co-culture system developed at LIST consisting of EA.hy926/A549/d.THP-1 cells and the liver model put forward was the HepG2 spheroid model developed by the PATROLS project at Swansea University (Llewellyn et al., 2020, Llewellyn et al., 2022). The selected models and endpoints were decided upon in conjunction with partners who could contribute experimental work to this Task; four independent laboratories (SU, NILU, IMI, and LIST) were chosen for each model. To ensure synergy between the experimental output of all tasks in WP5, the test ENMs utilised in Task 5.1 round robin-1 and -2 were chosen as the test materials for this experimental work.



## Critical Literature Review

Task 5.3 was initiated on the premise that we (WP5 partners) selected key organs of exposure which are highly relevant to ENM human hazard assessment. These organs were also strongly represented in the literature of advanced *in vitro* models and have featured in other ongoing Horizon 2020 projects. We then posed the question which of these advanced tissue models do we have experience with within the WP5 team? A pre-existing knowledge of these models was beneficial, allowing us to divide the literature among the partners and assign those with relevant expertise. This would also play heavily into our decision making when we arrived at the inter-laboratory transferability studies.

The first step was to summarise this information prior to any investigations into the literature was performed, this also allowed us to divide the critical review element of this task by having partners with experience with specific models to tackle the same test systems highlighted below in **Table 1**. The information summarised in Table 1 provided the foundations for Task 5.3 as it allowed us to spread the workload out across the partners. Table 1 also highlights areas of overlap where these models have proven to be successful in other Horizon 2020 projects currently running or which have recently been completed.

The selected advanced cell models highlighted in Table 1 were then used to initiate the critical review element of this task. First, the T5.3 team agreed-upon the key search criteria, the online databases, and the subsequent follow-up quality checking of the publications that we gathered and catalogued. Similarly, spreadsheets were designed by SU enabling partners to record important information on each publication which would later allow for models to be compared using cross-references of ENM type and biological endpoints.

The online databases which would be used to harvest the literature were based on partners accessibility to the platforms, however the source of the literature was either PubMed, Scopus, and/or Web of Science. Wherever possible we encouraged partners to assist each other if accessibility to a specific paper was unavailable by sharing links and PDFs so that the maximum number of high-quality papers could be gathered for the model comparisons. One key feature of Table 1 which would allow partners to streamline the search process was to focus upon the key biological endpoints which were examined in the publications. Maintaining a record of the biological endpoints allowed us to streamline paper returns in the online



databases by using them as key words in the search criteria. This then removed studies in which these endpoints were not focused upon.



**Table 1.** Summary of the advanced test systems in which the Task 5.3 contributing partners have experience with. Also summarised in Table 1 are the cell lines used to manufacture the advanced model as well as the biological endpoints and any overlap with other Horizon 2020 projects where standard operating procedures (SOPs) may be publicly available.

Tissue being modelled	Model	Cell Line(s) used	Group Affiliation	Biological endpoints evaluated by model	Overlap with other EU or national projects
Human Skin	1. Reconstructed human epiderm	1. Epiderm Tissues	1. Swansea University (SU)	1. Cytotoxicity, Genotoxicity, ENM Uptake by TEM	1. NA
	2. Co-culture	2. HaCaT keratinocytes & HFF-1 Fibroblasts	2. SU	2. Cytotoxicity (Trypan Blue Exclusion assay) – Previously used; MTT and LDH assay. (Pro)-inflammatory response	2. NA
	3. 3D Reconstructed human skin	3. RHS models	3. SU Procter & Gamble, BfR, Department of Chemical and Product Safety, Cosmetics Europe, Freie Universität Berlin, Institute for Pharmacy (Pharmacology and Toxicology)	3. Genotoxicity	3. NA
Lung	1. Co-culture	1. 16HBE14o- & d.THP-1	1. SU	1. Cytotoxicity, Genotoxicity, Immune response, Uptake by TEM	1. NA
	2. Co-culture	3. A549 & THP-1	3. SU	3. Cytotoxicity, Genotoxicity, Immune response	3. PATROLS



DELIVERABLE 5.4 | PUBLIC

	3. Air Liquid interface co-culture model (VibroCell Cloud)	5. A549 + EA.hy926 + THP-1	5. LIST & NILU	5. Cytotoxicity, Inflammation, genotoxicity, oxidative stress, uptake, and translocation	5. npSCOPE NanoBioReal
	4. Air Liquid interface co-culture model (VibroCell Cloud)	4. A549; Ea.hy926, THP-1 (macrophage-like), HMC.1	4. LIST	4. Cytotoxicity, Inflammation genotoxicity, oxidative stress, uptake, and translocation	4. npSCOPE
	5. Air Liquid interface co-culture model (VibroCell Cloud)	5. A549; Ea.hy926, THP-1 (macrophage-like), THP-1 (naïve - dendritic cells)	5. LIST	5. Cytotoxicity, Inflammation, respiratory sensitization, genotoxicity, oxidative stress, uptake, and translocation	5. NA
	6. Co-culture	6. 16HBE14o- + THP-1 + HLMVEC	6. KU LEUVEN	6. Inflammatory response	NA
<b>Gastro-Intestinal Tract</b>	1. Intestinal co-culture	1. Caco-2 and HT-29/MTX	1. LIST	1. Cytotoxicity, Inflammation, respiratory sensitization, genotoxicity, oxidative stress, uptake, and translocation	1. NanoHarmony
<b>Liver</b>	1. 3D Spheroids	1. HepG2	1. SU & NILU (hanging drops)	1. Cytotoxicity, Liver Function, Pro-inflammatory Response, Genotoxicity.	PATROLS, HISENTS
	2. 3D Spheroid co-culture	2. HepG2 & Human Kupffer Cells	2. SU	2. Cytotoxicity, Liver Function, Pro-inflammatory Response, Genotoxicity	NA
	3. 3D spheroids	3. HepaRG	3. ANSES	3. Cytotoxicity, genotoxicity	NA
<b>Brain</b>	1. Chicken embryo	1. Primary cortical neurons	1. NILU	1. Cytotoxicity	NA
	2. Co-culture	2. hCMEC & 1321N1	2. IMI	2. Cytotoxicity, Genotoxicity, Immune response, Uptake by confocal microscopy and flow cytometry; Mito Tracker, LysoTracker	2. SENDER (funded by the European Social Fund)



**DELIVERABLE 5.4 | PUBLIC**

<b>Lab on-a-chip biomimetic microfluidic platforms</b>	1. Monolayer	1. A549 cells	1. UiB	1. Viability, proliferation -live impedance and microscopy	1. GEMNS
	2. Microvasculature on-a-chip	2. Human microvascular endothelial, human vascular smooth muscle, human dermal fibroblasts	2. UiB	2. Transepithelial permeability, proinflammatory cytokines, viability transepithelial/trans endothelial electrical resistance	NA
	3. Lung and microvasculature on-a-chip	3. Human lung alveolar epithelial cells, lung microvascular endothelial cells	3. UiB	3. Trans endothelial permeability of 70KDa dextran, cell death by fluorescence microscopy.	3. NanoBioReal



The initial search terms used by each partner for their designated model tissue has been summarised below in **Table 2**. In the case that extreme numbers were returned by these initial searches, partners were free to streamline their searches with the addition of key search terms such as the biological endpoints stated in Table 1.

**Table 2.** A summary of the initial search terms used by each partner to initiate the critical review element of Task 5.3.

Partner	Initial Search Terms	Tissue being modelled
SU	Human epiderm AND nano*	Skin
NILU	A549 AND nano* primary cortical neuron AND nano*	Lung Brain
KU Leuven	16HBE14o- AND nano*	Lung
IMI NILU	hCMEC AND nano* HepG2 AND nano*	Liver
ANSES	HepaRG AND nano*	Liver
UiB	Human microvascular endothelial cell AND nano* Human vascular smooth muscle AND nano*	Microvasculature

At this stage in the task where we had established a methodology to extract papers from the literature, it was necessary to catalogue and store this data in relevant spreadsheets. The degree to which we agreed to harvest this information proved to be quite significant and three separate spreadsheets were developed for:

1. advanced *in vitro* models,
2. *in vitro* monoculture models, and
3. *in vivo* models.

Within each spreadsheet were common features which would later allow us to cross-check models in comparisons, allowing us to determine if the advanced test systems were more- or

less-predictive of *in vivo* ENM-induced toxicity than 2D *in vitro* models. Data extraction from the papers was achieved by populating Excel tables with the headings:

- nanomaterial
- source of nanomaterial
- primary particle size
- secondary particle size
- other physico-chemical characteristics
- sonication method
- dose range used
- exposure time
- exposure conditions
- cell type
- source of cell line
- seeding density
- assays used
- replicate number
- positive control data
- significant results
- author conclusions
- validity of the approach
- was interference considered
- reference to the paper
- GUIDEnano Q-Score.

Developed in conjunction with the data-extraction spreadsheets were the quality-control spreadsheets. The quality control measure used in Task 5.3 was the GUIDEnano process, first published in 2018 by Fernandez-Cruz *et al* (Fernández-Cruz et al., 2018). This method allows the publications to be scientifically critiqued and appraised based on their descriptions of both the ENM physico-chemical characterisation and by evaluating how well the biologically relevant details have been stated. The GUIDEnano methodology proved to be the most suitable approach for appraising the scientific quality of the papers collected in this task as a score can be awarded to each paper based on how much detail has been reported in the study. Briefly, the ENM physico-chemical characterisation can be awarded an S-Score and the biological content is awarded a K-Score, which when combined can only produce 1 out of 4 possible Q-Scores. Crucially, the GUIDEnano scoring process lists some criteria as essential and some non-essential, for example naming of the ENMI is essential but stating whether there was endotoxin contamination is non-essential to the final score. Here the T5.3 team agreed together that where the GUIDEnano specifies that ENM ‘Shape’ and ‘Purity’ are essential criteria, it was too restrictive for the purposes of this literature review and may have resulted in otherwise useful studies to be removed from our final selection. Therefore, we re-evaluated our scores to include publications which did not state the shape and / or purity of their test ENM.

Following the successful data extraction and GUIDEnano scoring of the advanced model studies, Task 5.3 was then steered towards performing a similar task for the 2D monocultured cell lines which were used in the advanced *in vitro* systems. Knowing that the number of publications would be significantly greater in the online databases for the less-advanced *in vitro* systems, a greater degree of care was given for the search criteria. To streamline the number of papers returns each partner used specific search criteria to focus on studies which included the same type of ENM utilised in the advanced models and covered similar endpoints as reported in the advanced model papers reviewed. The assays employed to measure the endpoint did not have to be the same (lactate dehydrogenase (LDH) vs. Alamar blue for example); however, a note of which assay used was archived in the Excel spreadsheet. A summary of the search criteria for each partner has been provided below in **Table 3**.

**Table 3.** A summary of the key search criteria for each partner's critical review of the literature on 2D *in vitro* monoculture models.

Monoculture Cell Line	Search Terms	Endpoints (derived from advanced model results)	Partner Responsible
HaCaT keratinocytes	HaCaT AND iron oxide nanoparticles HaCaT AND silver nanoparticles HaCaT AND titanium nanoparticles HaCaT AND aluminium nanoparticles	Cytotoxicity, genotoxicity, (pro)-inflammatory response	SU
HFF-1 Fibroblasts	HFF-1 AND iron oxide nanoparticles HFF-1 AND silver nanoparticles HFF-1 AND titanium nanoparticles HFF-1 AND aluminium nanoparticles	Cytotoxicity, genotoxicity, (pro)-inflammatory response	SU
16HBE14o-	16HBE14o- AND iron oxide nanoparticles 16HBE14o- AND CNTs	Cytotoxicity, genotoxicity, (pro)-inflammatory response	KU Leuven
A549	A549 AND ZnO nanoparticles A549 AND TiO <sub>2</sub> nanoparticles A549 AND Ag nanoparticles A549 AND CuO nanoparticles	Cytotoxicity, genotoxicity, (pro)-inflammatory response	NILU & LIST
Caco-2	Model not used	Model not used	Model not used
HT-29/MTX	Model not used	Model not used	Model not used
HepG2	HepG2 AND ZnO nanoparticles HepG2 AND TiO <sub>2</sub> nanoparticles HepG2 AND Ag nanoparticles HepG2 AND CuO nanoparticles	Cytotoxicity, genotoxicity, (pro)-inflammatory response	NILU
Primary cortical neurons	Model not used	Model not used	Model not used
hCMEC	hCMEC AND gold nanoparticles hCMEC AND iron oxide nanoparticles hCMEC AND arsinoliposomes	Cytotoxicity, genotoxicity, (pro)-inflammatory response	IMI
1321N1	Model not used	Model not used	Model not used
Human microvascular endothelial cell	HMEC-1 AND silver nanoparticles HMEC-1 AND silica nanoparticles HMEC-1 AND carbon nanotubes HUVEC AND silver nanoparticles HUVEC AND silica nanoparticles HUVEC AND carbon nanotubes	Cytotoxicity, oxidative stress, proliferation	UiB
Human vascular smooth	VSMC AND silver nanoparticles	Cytotoxicity, oxidative stress, proliferation	UiB





**DELIVERABLE 5.4 | PUBLIC**

muscle cell	VSMC AND silica nanoparticles VSMC AND carbon nanotubes		
HepaRG	HepaRG AND ZnO HepaRG AND TiO <sub>2</sub> HepaRG AND MWCNTs HepaRG AND AgNPs HepaRG AND CeO <sub>2</sub> HepaRG AND DQ12	Cytotoxicity, genotoxicity, (pro)-inflammatory response	ANSES



Following the data extraction and GUIDEnano scoring of the *in vitro* monoculture publications, the remaining element of this critical review of the literature was to focus on the *in vivo* data extraction from the literature to serve as the final comparison between the three model types. This *in vivo* literature search would again streamline the study returns and allow for direct comparisons by only extracting publications which utilised the same type of ENM, and similar biological endpoints which appeared in the two literature reviews performed prior. A summary of the *in vivo* search criteria, ENM type and biological endpoints have been detailed below for each partner (**Table 4**).

**Table 4.** Summary of the search criteria, the type of ENM and list of targeted endpoints for each partner to conduct the *in vivo* critical review of the literature.

In vivo tissue	Search Terms	Endpoints (derived from advanced model results)	Partner Responsible
Skin	In vivo AND skin AND iron oxide nanoparticle AND toxicity In vivo AND skin AND aluminium nanoparticle AND toxicity In vivo AND skin AND silver nanoparticle AND toxicity In vivo AND skin AND titanium nanoparticle AND toxicity	As paper number was small, no extra search criteria were used on biological endpoint	SU
Lung	In vivo AND lung AND TiO <sub>2</sub> AND toxicity In vivo AND lung AND γ-Fe <sub>2</sub> O <sub>3</sub> and Fe <sub>3</sub> O <sub>4</sub> ultrafine superparamagnetic iron oxide nanoparticles (dSPIONs) AND toxicity In vivo AND lung AND CeO <sub>2</sub> AND toxicity In vivo AND lung AND SiO <sub>2</sub> AND toxicity In vivo AND lung AND DQ12 AND toxicity In vivo AND lung AND MWCNTs AND toxicity In vivo AND lung AND AuNPs AND toxicity In vivo AND lung AND CuO AND toxicity	Cytotoxicity, uptake, genotoxicity, inflammation	KU Leuven & NILU
Liver	In vivo AND liver AND ZnO In vivo AND liver AND AgNP In vivo AND liver AND MWCNT In vivo AND liver AND TiO <sub>2</sub> In vivo AND liver AND CeO <sub>2</sub> In vivo AND liver AND DQ12	Cytotoxicity, uptake, genotoxicity, inflammation	ANSES
GI Tract	Model not used (time inefficient)	Model not used	Model not used
Brain	In vivo AND brain AND AuNP In vivo AND brain AND SiO <sub>2</sub> In vivo AND brain AND Fe <sub>3</sub> O <sub>4</sub> In vivo AND brain AND AgNP In vivo AND brain AND TiO <sub>2</sub>	Cytotoxicity, uptake, genotoxicity, inflammation	IMI
Microvasculature	In vivo AND vasculature AND nano* AND toxicity	As paper number was small, no extra search criteria were used on biological endpoint	UIB



Following the collection of the literature material we now possessed ENM toxicity data pertaining to each organ of interest (relevant to ENM exposure, which are strongly represented in the literature) depicted in advanced *in vitro* models, standard 2D *in vitro* monocultures and *in vivo* testing systems. The aim of the next step was to compare the data from the advanced models against the *in vivo* data to judge how representative the more complex *in vitro* systems are. This comparison was performed by using models which utilised the same ENM type and same biological endpoints. The grounds for these comparisons were based on the following presupposition:

*Does the advanced in vitro study report the same outcome as seen in vivo?*

An example of this comparison has been outlined below with one example from the skin performed by SU, where the effects seen *in vivo* against an advanced model with iron oxide as the test ENM were compared (**Table 5**). In the model comparison it was important to note key features in each study such as any significant toxicity, and where observed, what the initial significant dose was. If there were no significant data points, then partners were encouraged to indicate this in their comparison spreadsheets. Finally, a concluding colour coded format was applied to the spreadsheet: if there was disagreement between the models the colour code would be white; if there was agreement between the models a blue was applied; and if there was no clear evidence of correlation between *in vivo* and advanced *in vitro* this would be yellow.

To determine whether the advanced *in vitro* models represented valid improvements over the standard 2D monoculture models a second spreadsheet was designed to accommodate this comparison. The spreadsheet format was the same as for the *in vivo* comparison however the new presupposition was:

*Was the advanced model an improvement over the standard in vitro model?*

Here partners again performed a one-to-one model comparison providing scientific rationale for their decision making to determine whether the advanced models can more closely mimic the responses observed *in vivo* as compared to the 2D monocultures, thereby showing they are valid improvements over the less-advanced test systems. This was performed as detailed above in the first comparison – by using studies from the literature which utilised the same type of ENM and corresponding endpoints.

**Table 5.** Summary table detailing how the advanced *in vitro* models were compared against the *in vivo* models. A brief description of the model was provided with the corresponding reference and modified Q-Score. Partners then provided rationale for their decision making in the final column explaining their comparisons. The modified Q-Scores proved useful when studies appeared to disagree, but one had a high Q-Score whilst the other had a low Q-Score.

Description of advanced model & state the ENM being compared	Reference for advanced model	MODIFIED Q Score Advanced model	Description of <i>in vivo</i> model & state the ENM being compared	Reference for <i>in vivo</i> model	MODIFIED Q Score in vivo model	Does the advanced <i>in vitro</i> paper report the same outcome seen <i>in vivo</i> ?
The EpiDerm™ consists of normal human-derived keratinocytes, multiple viable cell layers, and functional stratum corneum.  <b>Fe<sub>2</sub>O<sub>3</sub>/Fe<sub>3</sub>O<sub>4</sub> NPs</b>	Skin Corrosion and Irritation Test of Nanoparticles Using Reconstructed Three-Dimensional Human Skin Model, EpiDerm™. <i>Toxicol Res</i> , 32, 311-316.	<b>0</b>	The animals used in the study were adult female and male SKH-1 hairless mice.  <b>Fe<sub>3</sub>O<sub>4</sub></b>	Biocompatible Colloidal Suspensions Based on Magnetic Iron Oxide Nanoparticles: Synthesis, Characterization and Toxicological Profile. <i>Front Pharmacol</i> , 8, 154.	<b>0</b>	Significant cytotoxicity after 3 and 60 minutes in advanced model for skin corrosion test. ENMs negative for skin irritation test. No significant changes to viability <i>in vivo</i> when exposed to Fe <sub>3</sub> O <sub>4</sub> at 5, 10, 25ug/ml over 24 hours.



Once all the collected models had been compared with one another in the final spreadsheet, we evaluated which models would be feasible to take forward into a small ring trial within the RiskGONE WP5 team. This provided us with a shortlist of advanced *in vitro* models which could potentially be taken forward into a small inter-laboratory trial. From the comparisons between the models, we discovered that whilst the *in vitro* monocultures tended to have the higher Q-Score, the advanced *in vitro* models did show a marked improvement in mimicking human tissue. There were also a significant number of study returns for both the liver and the lung for advanced models which have been well-established in the literature. These studies however did tend to score lower in the GUIDEnano criteria due to the emphasis in the studies being on model development and characterisation, but less so on the ENM characterisation – which was the overwhelming reason a study would score below 0.5 (acceptable quality).

For the liver publications, the HepG2 SOP developed by SU in the PATROLS project appeared as a highly robust and scientifically validated method for testing ENM human hazard assessment in a liver advanced *in vitro* system (Llewellyn et al., 2020). The operating protocol had been established and published, multiple partners have had cell culture experience with the HepG2 cell line (which is used to form the spheroids), and the proposed ENMs have already been tested thoroughly in earlier RiskGONE round robin exercises. The proposed lung model was developed at LIST and has also been published in recent years. This model is an A549/Ea.hy926/THP-1 triple cell model for which LIST have prepared an updated handling protocol. Other models shortlisted were for the GI tract, the brain and lab-on-a-chip microfluidic systems however the WP5 team concluded that these would be highly specialised requiring either additional time or finances to incorporate into Task 5.3. From the list of models, we decided that the lung and liver models would be best suited as the operating protocols were freely available and the experimental expertise of the WP5 partners were best suited to these two advanced *in vitro* models (**Table 6**). In addition, extra experiments were performed on 2D and 3D HepaRG cells by ANSES to compare the viability and genotoxicity results of 3 different ENMs.

**Table 6.** Final model selection for the experimental work performed in Task 5.3.

Tissue being modelled	Advanced Model	Endpoint & Assay Employed	Partner(s)	Nanomaterials	Exposure Time (h)	Concentrations	Sonication
Lung	LIST Lung Model: A549/EA.hy926/THP-1	Cytotoxicity (Alamar Blue)  Inflammatory Response (IL-8 ELISA)	SU LIST NILU	PlasmaChem (PL-CuO) CuO (ERM00000088)  NM105 TiO <sub>2</sub> (erm:ERM00000064) Triton X-100 Positive control for cytotoxicity. LPS Positive inflammatory marker	24	Negative control (Saline (0.9% NaCl)) CuO, 1000 ng/cm <sup>2</sup> TiO <sub>2</sub> , 1000 ng/cm <sup>2</sup> Triton X-100, 1% LPS, 1ug/ml	LIST SOP
Liver	PATROLS Liver Model: HepG2 Spheroids	Cytotoxicity (Trypan Blue)  Inflammatory Response (IL-8 ELISA)	SU  IMI  NILU	PlasmaChem (PL-CuO) CuO (ERM00000088)  NM105 TiO <sub>2</sub> (erm:ERM00000064) MMS Positive chemical control for cytotoxicity. LPS Positive inflammatory marker	24	CuO, 0, 0.25, 0.5, 1, 2 µg/ml JRC TiO <sub>2</sub> , 0, 10, 25, 50, 100 µg/ml MMS, 2 µg/ml LPS, 1 µg/ml	LIST SOP
	ANSES protocol (Mandon et al 2019) HepaRG spheroids In comparison with the 2D HepaRG cultures	Cytotoxicity (ATP)  Comet assay with and without Fpg	ANSES	NM105 TiO <sub>2</sub>  ZnO ENM from Sigma (ERM00000063)  NM110 ZnO  MMS and KBrO <sub>3</sub> for positive controls	24h for ZnO and 48h for TiO <sub>2</sub>	0.1, 1, 5, 10, 25, 50 and 100 µg/mL corresponding respectively to 0.031, 0.31, 1.5625, 3.125, 7.8125, 15.625 and 31.25 µg/cm <sup>2</sup>	LIST SOP NanoGenoTox SOP



## Results of inter-laboratory experimental work

Following on from the completion of the systematic review of the literature, the two advanced *in vitro* models taken forward for round robin testing focused upon the lung and the liver. The models selected and can be seen in Table 6 were a co-culture of A549, EA.hy.926 and differentiated THP-1 macrophages to represent the alveolar region of the lung, and the liver model consisted of HepG2 spheroids. The operating protocols and culturing techniques used for each model were provided by the PATROLS project (detailing the HepG2 spheroids) and by LIST (detailing the tri-culture model of the lung). The ENMs utilised for the 24-hour exposures were selected based upon the results obtained from Task 5.1 whereby a non-cytotoxic material (TiO<sub>2</sub>) and a strong cytotoxic material (CuO) could be evaluated again, but in two advanced *in vitro* models. The exposure concentrations used in the HepG2 spheroids were linked to the concentrations used in Task 5.1. To benefit from the work conducted in other Horizon 2020 EU projects, when deciding on the exposure concentrations to use in the lung model we followed on from the lung model research of the PATROLS project. Here, we selected 1000 ng/cm<sup>2</sup> as our exposure concentration delivered by the VitroCell. Detailed below are the results reported for the advanced *in vitro* liver models delivered by SU and IMI (NILU data in preparation). Furthermore, experimental data has been generated using the triculture originally developed by at LIST which consists of A549 alveolar epithelial cells, EA.hy926 endothelial cells and differentiated THP-1 macrophages. The lung model data was generated in an interlaboratory trial involving SU, LIST and NILU (data in preparation).





### Advanced Liver Model Data

The HepG2 spheroid model developed in the PATROLS project was utilised as the most valid advanced 3D liver model to conduct ENM exposures with. The two materials selected were TiO<sub>2</sub> (selected as a negative cytotoxic material) and CuO (positive cytotoxic material), both were exposed to HepG2 spheroids for 24-hours. The HepG2 spheroids would be exposed to each ENM and evaluated for cytotoxicity and the induction of a (pro)-inflammatory response using the trypan blue exclusion assay and an IL8 ELISA respectively. Suitable positive cytotoxic and (pro)-inflammatory controls of methyl methanesulfonate (MMS) and lipopolysaccharide (LPS) were selected respectively.

Following 24-hour exposure to TiO<sub>2</sub> no significant cytotoxicity was observed at any test concentration, this was consistent in both laboratories (**Figure 1A**). However, statistically significant depletion in cell viability of HepG2 spheroids was observed following MMS exposure; this was consistent in both laboratories with approximately 50-60% reduction in viable cells. Supernatants harvested from the spheroids post-exposure revealed no change in IL8 levels from baseline concentrations of 94.4 pg/ml. There was further concordance observed between both laboratories for the LPS control which induced a statistically significant increase in IL8 by 12-fold. As with data reported in Task 5.1 the CuO ENM induced statistically significant cytotoxicity in HepG2 spheroids. The dose-response trends between the laboratories were almost identical. However, there was a subtle difference observed in the initial concentrations in which a significant drop in cell viability was detected. At laboratory 1 the only concentration which induced a significant depletion in cell viability was 2 µg/ml at which viability dropped to 44% whereas at laboratory 2, a concentration of 1 µg/ml reduced the viability to 61% (**Figure 1B**). Nonetheless, the absolute figures (raw data) were very similar between laboratories, with some slight variation in replicates resulting in the marginal differences in statistical significance. In summary, high levels of concordance were observed between the two laboratories for both cytotoxicity and (pro)-inflammatory endpoints using the 3D liver spheroids and following 24-hour exposures to ENM and positive controls. It is also notable that background, negative control datasets were almost identical between the laboratories, demonstrating excellent transferability of the in-house 3D model construction.

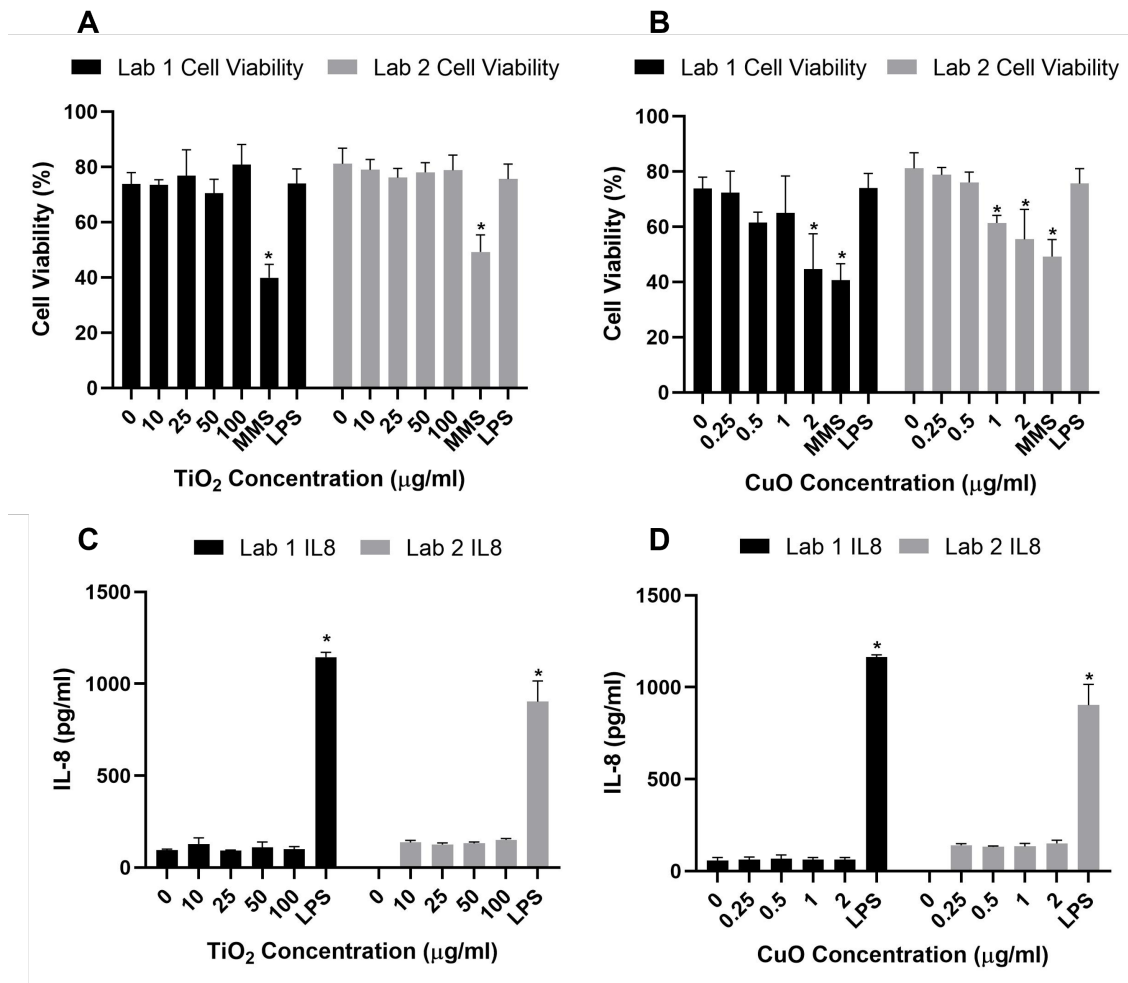


**Figure 1.** Results of the HepG2 spheroid interlaboratory experiments following a 24-hour exposure to TiO<sub>2</sub> and CuO ENMs. Cell viability determined via Trypan blue exclusion for TiO<sub>2</sub> is represented in panel **A** and CuO in panel **B** respectively. The results of the (pro)-inflammatory experiments are displayed for TiO<sub>2</sub> in panel **C** and CuO in panel **D**. Data shown in the average +/- the standard deviation, data was considered statistically significant when (\*) was p≤0.05 (n=3).

### Advanced Lung Models

To conduct the advanced *in vitro* lung model exposures, we followed on from the research conducted in the PATROLS project. Briefly, the concentration of 1000 ng/cm<sup>2</sup> was selected based upon the VitroCell exposures conducted with the same NM105 (TiO<sub>2</sub>) material used in this experimental work, albeit a different batch. Therefore, the same concentration was used for the CuO ENM. The exposure period was for 24-hours, and a deposition curve was conducted for the materials prior to conducting the exposures.

Prior to triculture exposures to each ENM, a quick calibration was required of the VitroCell cloud exposure system. Given that the TiO<sub>2</sub> had been previously characterised in the PATROLS project, a simple *N* of one was performed to check the deposition at three different stock concentrations (125, 250 and 500 µg/ml). As the CuO had never been applied to the VitroCell cloud in PATROLS, this was calibrated for an *N* of three (**Figure 2**). The negative control consisting of saline solution (0.9% NaCl) was also deposited for an *N* of three.

The exposure depositions achieved during the biological exposures to each material has been plotted below to provide an indicator as to the concordance between the two laboratories (**Figure 3**). Both laboratories showed a high degree of overlap with respect to the ENM deposition rates over the biological replicates. However, there appeared to be a significant difference when exposing the triculture to the negative control of 0.9% saline solution.

Following the 24-hour ENM exposures, the tricultures were evaluated for cell viability and (pro)-inflammatory response utilising the Alamar blue and IL8 ELISA respectively (**Figure 4**). To maintain a strong link with the PATROLS, project the same ELISA assay kit was used for the RiskGONE evaluation. Within the cell viability assay, some concordance was observed for both laboratories for the negative control, the incubator control, and the exposure to TiO<sub>2</sub> ENM. However, whereas laboratory 1 observed a significant reduction in cell viability following CuO ENM exposure (approximately 50% reduction in viable cells), this effect was not observed in laboratory 2. Similarly, whilst the positive control of Triton X-100 reduced cell viability to approximately 50% in laboratory 1, at laboratory 2 this concentration resulted in total cell lethality. The quantification of a (pro)-inflammatory response was conducted on the cell supernatant (basal supernatant + apical wash) following the 24-hour exposure (**Figure 4B**). In both laboratories, a lack of (pro)-inflammatory response was observed with only the

positive control of LPS inducing a significant response. There were, however, differences reported in the laboratories with lab 1 demonstrating an LPS response (induction of IL8) from the triculture of ~5000 pg/ml whereas in lab 2 this effect was noticeably higher at ~13000pg/ml of IL8.

Laboratory 2 also conducted assay interference for the Alamar Blue cell viability assay which has been summarised below in **Figure 5**. Given laboratory 1 conducted this work in the Task 5.1 data packages for the comet assay supporting viability data, this was not performed for Task 5.3. However, as has been shown in Task 5.1 by laboratory 1 among all other contributing partners, there appears to be little-to-no ENM interference with the Alamar blue cell viability assay.

### VitroCell Deposition curves at SU

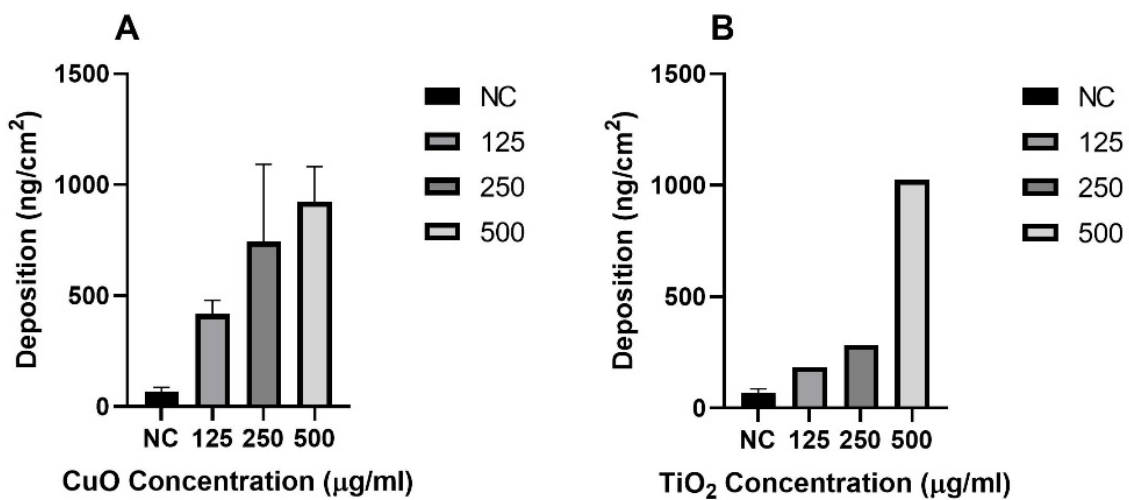


**Figure 2.** Deposition curves obtained for TiO<sub>2</sub> and CuO ENMs using stock concentrations of 125, 250, and 500 µg/ml. A biological *n*=1 was performed for TiO<sub>2</sub> as this material had been extensively characterised using the VitroCell under the PATROLS project. A biological *n*=2 was conducted for CuO ENM and a biological *n*=3 conducted for the negative control of filter-sterilised, distilled water spiked with 0.9% sodium chloride (NC).

### VitroCell Exposure Deposition

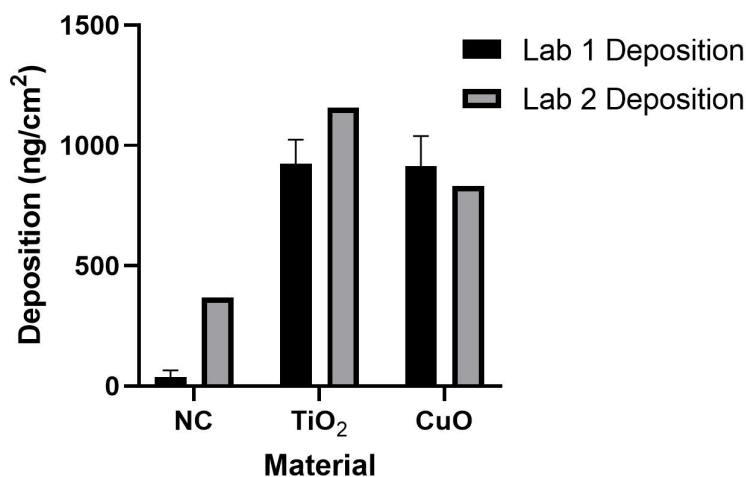


**Figure 3.** Exposure deposition achieved for both TiO<sub>2</sub> and CuO ENMs onto A549/EA.hy926/d.THP-1 lung co-cultures. A biological *n*=3 was conducted for the exposures.

### Endpoint data

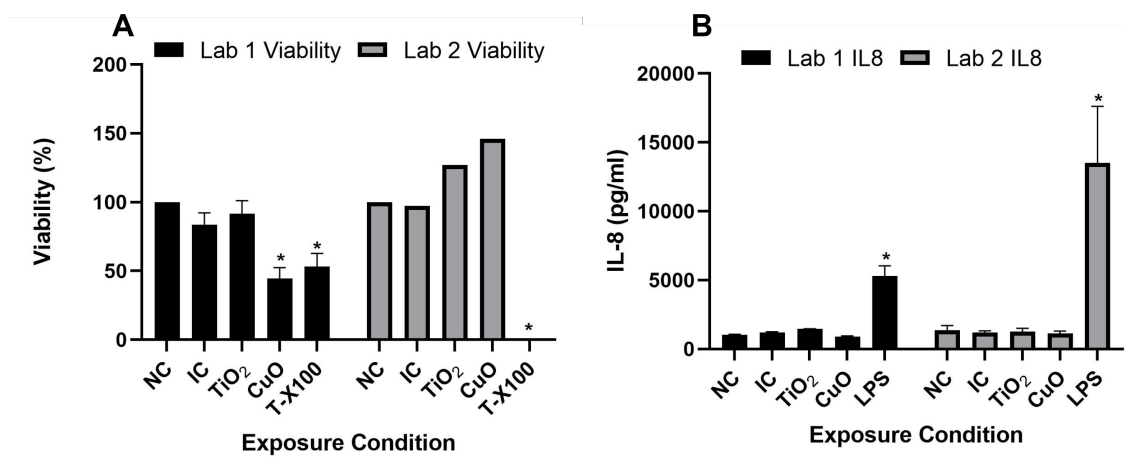


**Figure 4.** Measure of cytotoxicity and (pro)-inflammatory response following 24-hour exposure to TiO<sub>2</sub> and CuO ENMs. The positive controls used in each respective endpoint (cell viability, A and IL8 production, B) were Triton X-100 (1%) and LPS (1µg/ml). Data presented is the average +/- the standard deviation, data was considered statistically significant when (\*) was *p*<0.05, (*n*=3).

**ENM-assay interference-check at LIST**

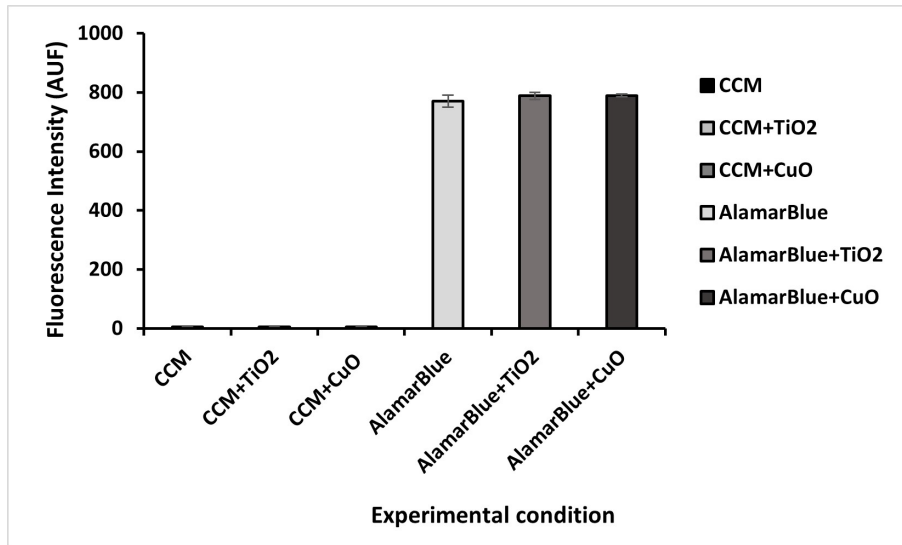


**Figure 5.** Measurements of Fluorescence Intensity (AUF) on TiO<sub>2</sub> and CuO ENM suspensions prepared in cell culture medium or Alamar Blue solution (AB final concentration 400mM, ENM final concentration equal to expected max deposition). Data presented is the average +/- the standard deviation, data was considered statistically significant when (\*) was  $p < 0.05$ , ( $n=3$ ).

### Experimental work on HepaRG cells conducted at ANSES

The protocol for using HepaRG 3D spheroids in the comet assay was developed by Mandon *et al* (2019).

### Advanced 3D HepaRG liver model

#### *Cytotoxicity (ATP measurement)*

TiO<sub>2</sub> ENM had no effect on cell viability of HepaRG cells grown in 3D, after a 48h treatment (Figure 6A). After a 24h treatment with aq. ZnO ENM, a decrease in cell viability at 50 µg/mL (around 72% of control value) was observed (**Figure 6B**). By contrast, treatment with NM110 did not significantly change cell viability (**Figure 6C**).

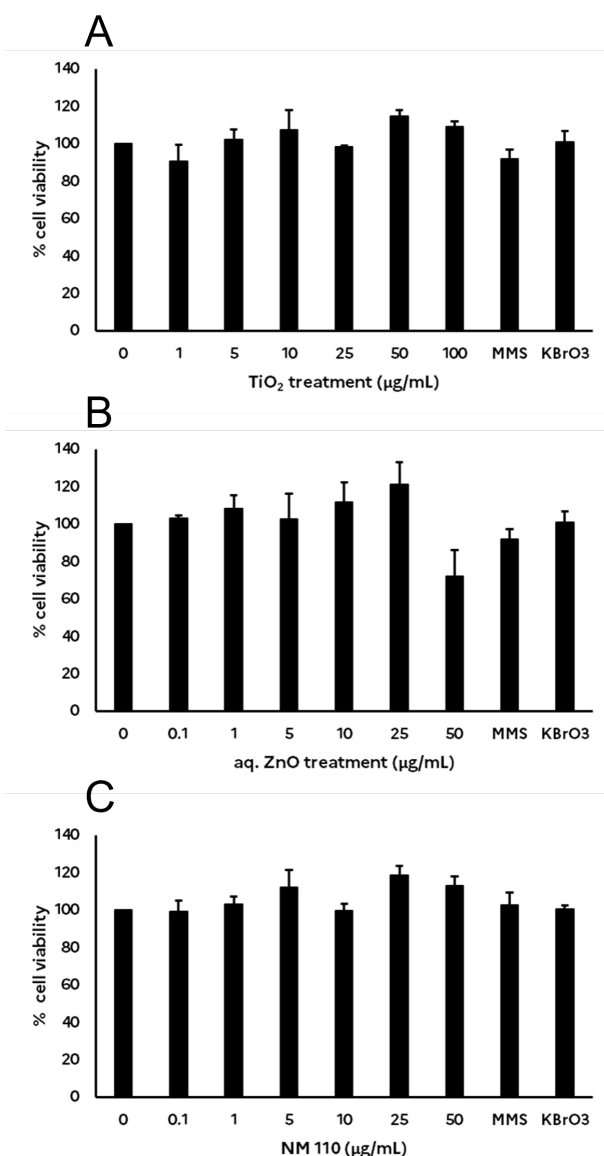


**Figure 6.** Cytotoxicity of 3D HepaRG cells, assessed by ATP measurements. Spheroids were treated with the positive controls (MMS and KBrO<sub>3</sub>) for 24h or the three ENMs: TiO<sub>2</sub> for 48h (panel A), aq. ZnO and NM110 for 24h (respectively panels B and C). Results are expressed as mean percentage cell viability compared to control +/- SEM, from four independent experiments. Statistical analysis was performed for each treatment compared to the negative control.



In the Comet assay experiment TiO<sub>2</sub> ENM treatment for 48h did not significantly modify the % Tail DNA, although a small increase was noticed at 100 µg/ml, in the absence of Fpg (**Figure 7A**). No effect on the % of hedgehogs was observed upon TiO<sub>2</sub> ENM treatment (**Figure 7B**). Both ZnO ENM induced a concentration-dependent increase in the % Tail DNA, very weak at 25 µg/ml but statistically significant at 50 µg/mL in both enzyme conditions for aq. ZnO ENM and only in the presence of Fpg for NM110 (**Figure 7B & C**). Both ZnO ENM also induced a concentration-dependent increase in the % of hedgehogs from 25 µg/ml, but this effect was statistically significant only at 50 µg/ml for aq. ZnO (**Figure 7E & F**). Again, the effects observed seemed slightly stronger for aq. ZnO than for NM110 ENM. Finally, no clear effect on net Fpg sites could be detected upon treatment with the various ENMs.

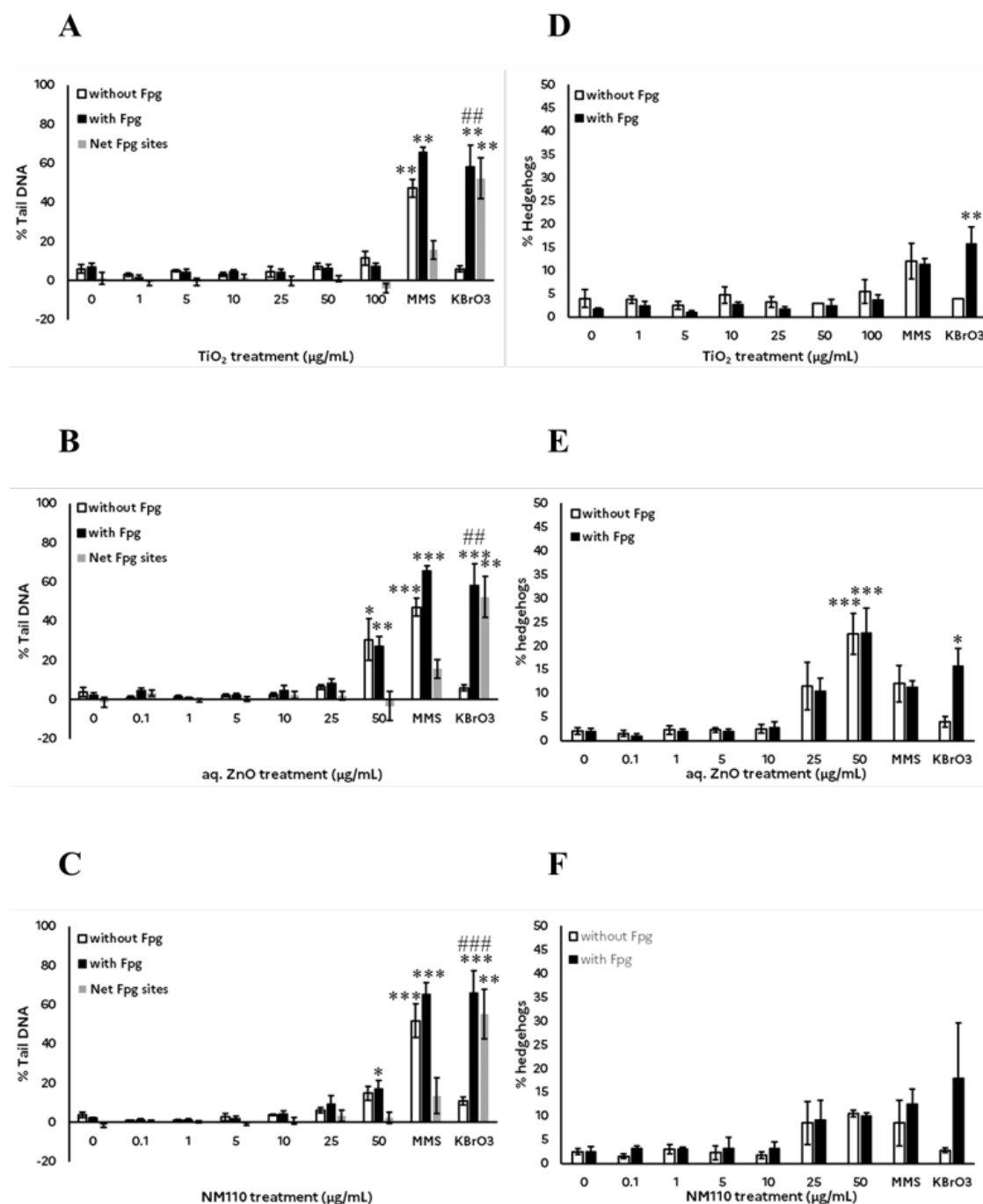


**Figure 7.** Genotoxicity testing in HepaRG cells grown in 3D, using the comet assay. Spheroids were treated with medium only (negative control) or with the positive controls (MMS and KBrO3) for 24h or with the three ENMs: TiO<sub>2</sub> for 48h or aq. ZnO and NM110 for 24h. Afterwards, spheroids were collected, and the comet assay was performed with or without the Fpg enzyme. Results are expressed as mean median % Tail DNA +/- SEM (panels A, B and C),

from four independent experiments. In parallel, the percentage of hedgehogs was also analysed and is represented as mean % of hedgehogs +/-SEM (panels: D, E and F). Statistical significance is indicated by \*  $p \leq 0.05$ , \*\*  $p \leq 0.01$  and \*\*\*  $p \leq 0.001$  compared to the respective controls with and without Fpg and # #  $p \leq 0.01$ , # # #  $p \leq 0.001$ , compared to the same treatment with and without Fpg.

## 2D HepaRG model

### *Cytotoxicity (ATP measurement)*

The  $\text{TiO}_2$  ENM treatment for 48h had no effect on the level of ATP measured in HepaRG cells grown in 2D (**Figure 8A**). By contrast, a concentration dependent decrease in ATP levels was measured upon treatment with aq. ZnO ENM, for 24h, from 25  $\mu\text{g/ml}$ , with more than 30% decrease compared to control (**Figure 8B**). Similarly, a concentration-dependent decrease in ATP levels was observed following NM110 treatment of HepaRG cells, for 24h, from 25  $\mu\text{g/ml}$ , with a 30% cytotoxicity reached only at 50  $\mu\text{g/ml}$  (**Figure 8C**).

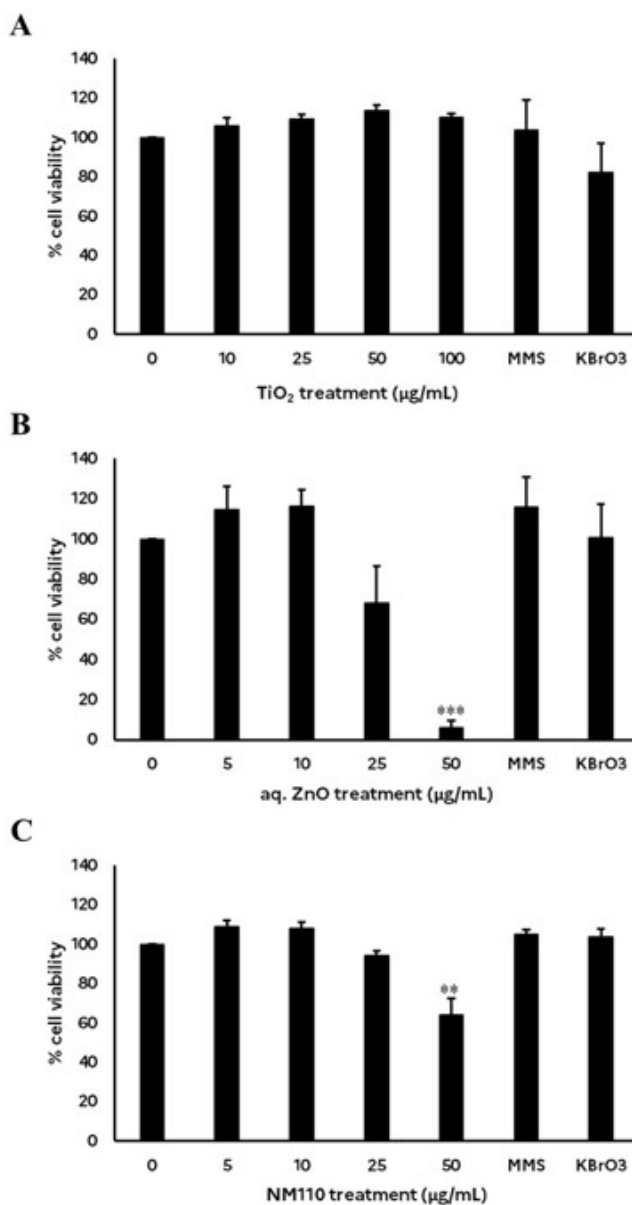


**Figure 8.** Cytotoxicity of 2D HepaRG cells, assessed by ATP measurements. Cells were treated with the positive controls (MMS and KBrO3) for 24h or with the three ENMs: TiO<sub>2</sub> for 48h (panel A), aq. ZnO and NM110 for 24h (respectively panels B and C). Results are expressed as mean percentage of cell viability compared to control +/- SEM, from at least two independent experiments, performed with technical duplicates. Statistical significance is indicated by \*\*  $p \leq 0.01$  and \*\*\*  $p \leq 0.001$  when treatment was compared to the negative control.

*Comet assay*

The TiO<sub>2</sub> ENM did not significantly modify the % Tail DNA in treated HepaRG cells and had no noticeable effect on the % of hedgehogs (**Figure 9A & D**). In contrast, both ZnO ENMs induced a concentration-dependent and a significant increase in the % Tail DNA at 25 and 50 µg/ml (**Figure 9B & C**). A similar observation was done on the percentage of hedgehogs (**Figure 9E & F**). Nevertheless, aq. ZnO ENMs seemed to induce slightly more effects than NM110 ENMs, in the comet assay. Finally, for all ENMs tested, no clear difference could be evidenced between the conditions with and without Fpg, except for NM110 at 50 µg/ml, which induced significantly more net Fpg sites than control. Importantly, for aqueous (aq.) ZnO ENM at 50 µg/mL, the signal for % Tail DNA was close to saturation (above or at the same level of positive controls).



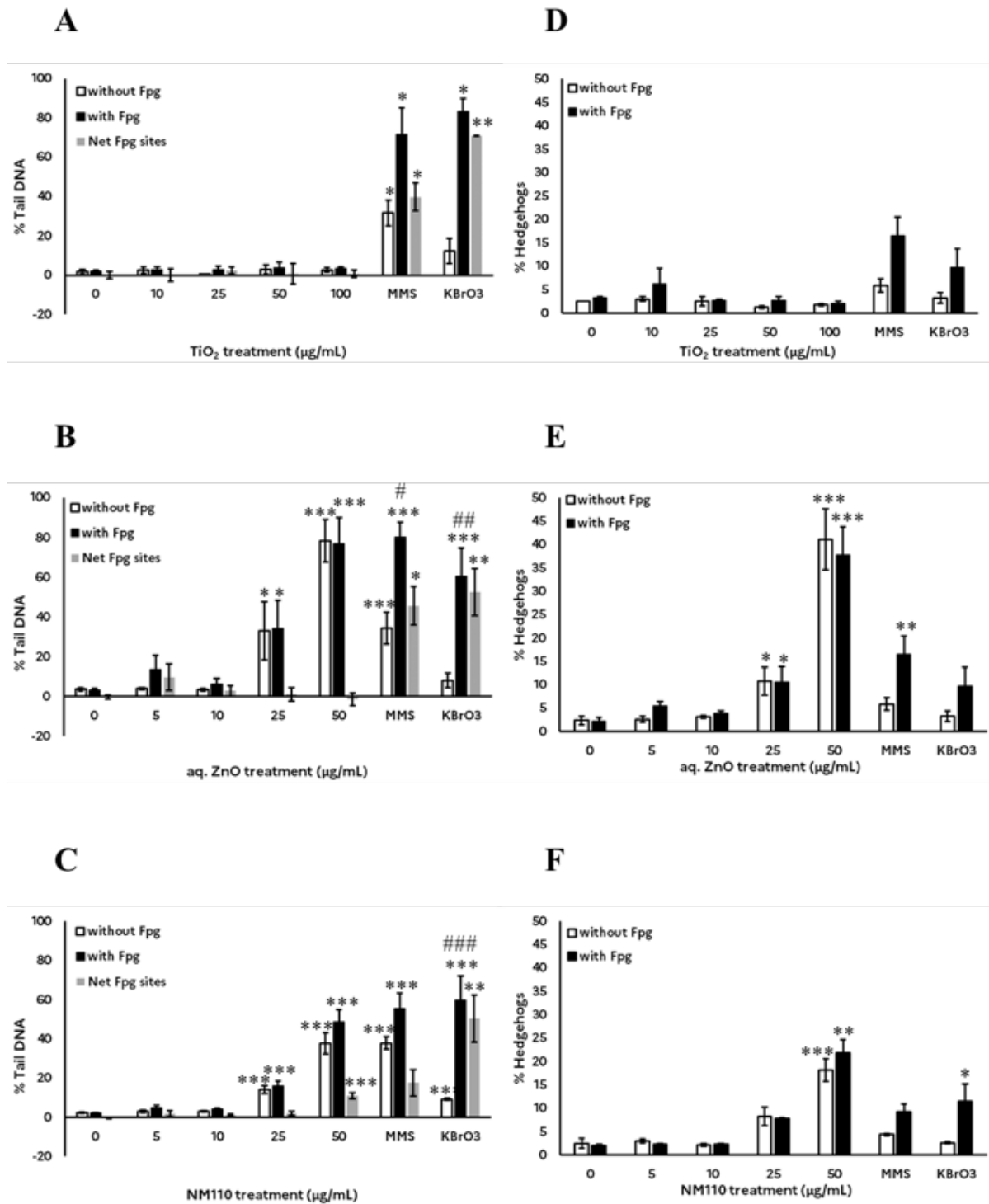


**Figure 9.** Genotoxicity testing in HepaRG cells grown in 2D, using the comet assay. Cells were treated with medium only (negative control) or with the positive controls (MMS and KBrO3) for 24h or with the three ENMs: TiO<sub>2</sub> for 48h or aq. ZnO and NM110 for 24h. Afterwards, cells were collected, and the comet assay was performed with and without the



Fpg enzyme. Results are expressed as mean median % Tail DNA +/- SEM (panels: A, B and C). In parallel, the % of hedgehogs was also analysed and is represented as mean % of hedgehogs +/-SEM (panels: D, E and F). Two independent experiments were performed with TiO<sub>2</sub> ENM while four independent experiments were performed with ZnO ENM. Statistical significance is indicated by \* p≤0.05, \*\* p≤0.01 and \*\*\* p≤0.001 compared to the respective controls with and without Fpg and # p≤0,05, # # p ≤0,01, # # # p ≤0,001, compared to the same treatment with and without Fpg.

### ENM-assay interference-check at ANSES

#### Cytotoxicity

The results indicated that, in the experimental conditions used, the three ENMs at the highest concentration tested did not interfere with the level of ATP measured neither in the 2D nor in the 3D cell cultures (**Figure 10**).

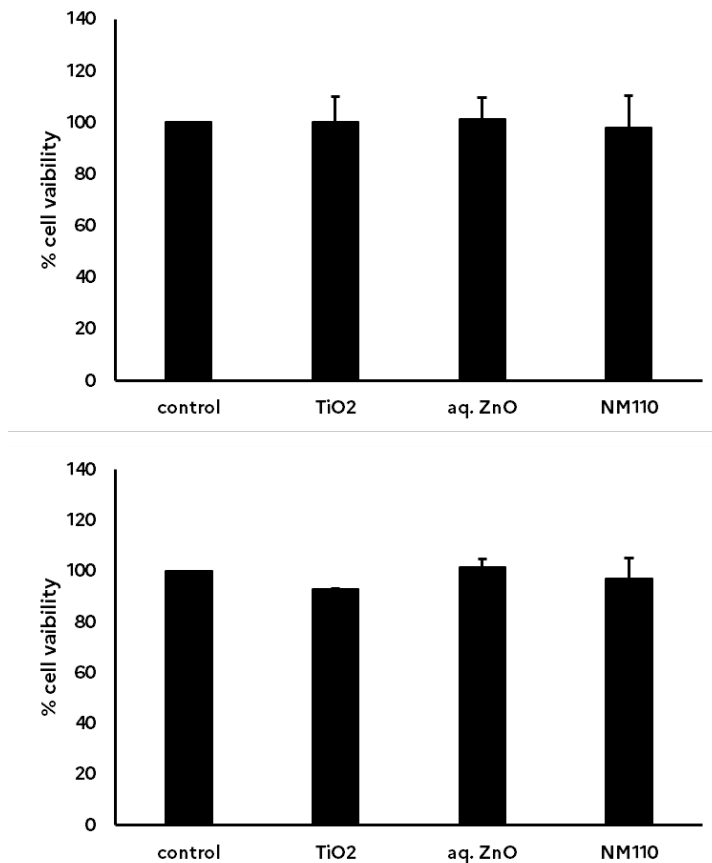


**Figure 10.** Tests for ENMs interference with the ATP measurement. Just before ATP analysis, cells were incubated with medium only (negative control) or with the three ENMs at the

highest concentration studied, on either HepaRG cells grown in 2D (panel A) or in 3D (panel B). Results are expressed as mean percentage cell viability compared to control +/- SEM, from two independent experiments.

### Testing for Interference in the comet assay

For interference testing, HepaRG cells grown in 2D were treated with MMS (100µM) or KBrO<sub>3</sub> (2mM) or incubated with medium only for control, for 3h. The time point of 3h was chosen so that the signal measured in the comet assay are either low or medium, but never saturated. Subsequently, cells were processed for the comet assay as already described, except that following mixing with LMP agarose, water control or ENMs resuspended in stock suspension (2.5mg/ml) were added and mixed (final concentration 100 µg/mL TiO<sub>2</sub> ENM or 50 µg/ml ZnO ENM) (Figure 11).

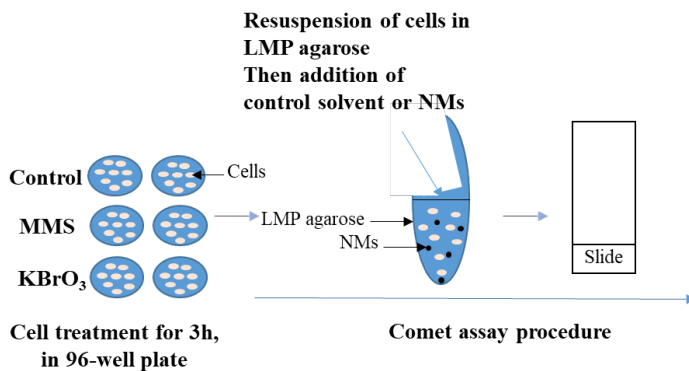


**Figure 11.** Schematic procedure to test for potential interferences of ENMs in the comet assay.

Results of interference testing with the comet assay are presented in Figure 12. In the absence of Fpg, only MMS treatment induced a significant increase in the % Tail DNA compared to control. The presence of ENMs into the gel did not significantly alter the level of the % Tail DNA compared to the respective conditions without ENMs (control, MMS or KBrO<sub>3</sub> alone). In the presence of Fpg, the % Tail DNA significantly increased with MMS and KBrO<sub>3</sub> These results treatments compared to the same conditions without Fpg, suggesting that oxidative base damage was clearly evidenced (Figure 12A). However, for cells treated with MMS and KBrO<sub>3</sub>, in the presence of TiO<sub>2</sub> and aq. ZnO ENM, a small but non-significant



decrease in the % Tail DNA could be observed only with Fpg, when comparing the corresponding conditions without ENMs. These results suggested that TiO<sub>2</sub> and aq. ZnO ENM slightly interfered with the Fpg step of the assay (**Figure 12A**). Regarding hedgehogs, a small but non-significant increase was observed upon MMS treatment. However, the presence of ENMs did not significantly modify the % of hedgehogs recorded with the various treatments, with and without Fpg (**Figure 12B**).

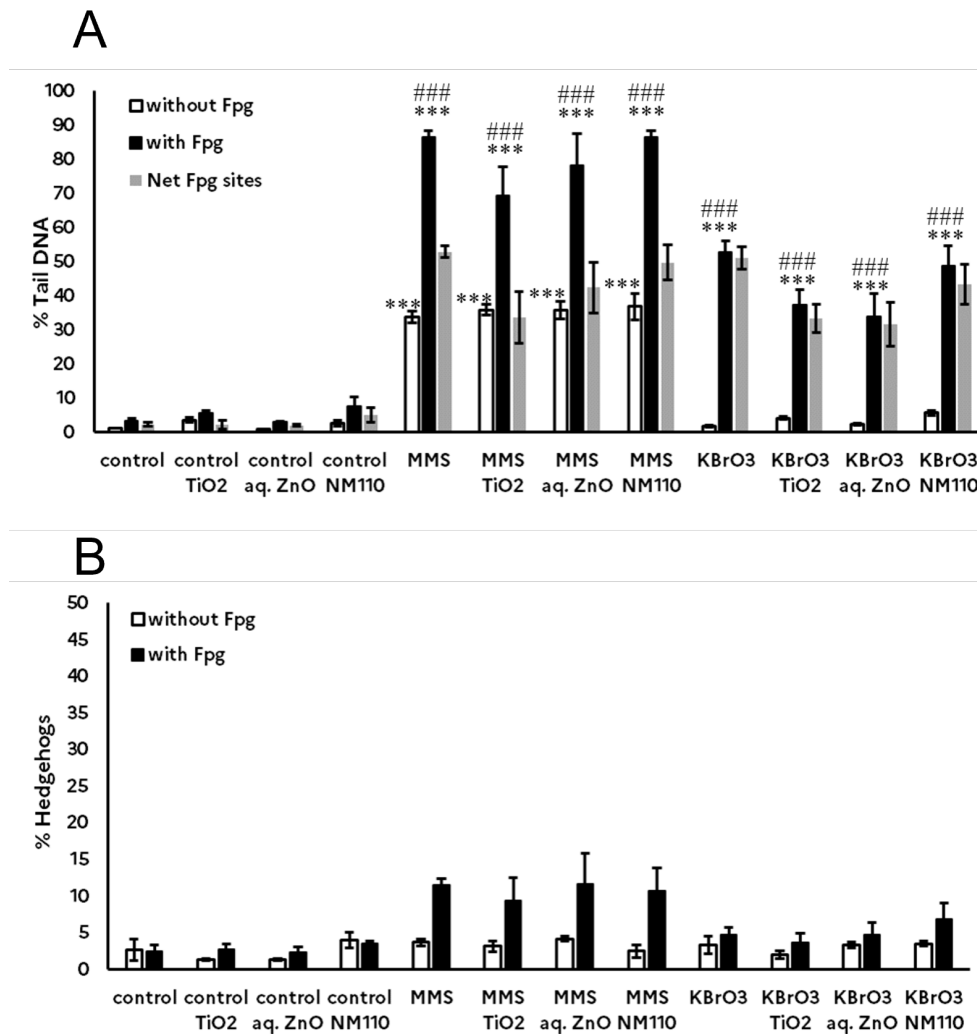


**Figure 12.** Tests for ENMs interference with the comet assay. Cells were untreated or treated for 3h with the positive controls (MMS and KBrO<sub>3</sub>) and prepared for the comet assay. ENMs were directly added into the LMP agarose containing the cells, at 100 µg/mL for TiO<sub>2</sub> and 50 µg/mL for ZnO ENM. The comet assay and cell scoring were subsequently carried out as previously described. Results are expressed as mean median % Tail DNA +/- SEM (panel A)

and mean % of hedgehogs +/-SEM (panel B), from three independent experiments. Statistical significance is indicated by \*\*\*  $p \leq 0.001$  compared to the respective controls with and without Fpg and # # #  $p \leq 0.001$ , compared to the same treatment with and without Fpg. Comparisons and statistical analyses were also performed for control, MMS and KBrO<sub>3</sub> conditions in the absence and in the presence of the respective ENMs.

## Conclusions

### Advanced Liver Models

#### Endpoint data

The data generated by both laboratories concerning the HepG2 spheroid models showed a high degree of concordance for both measured endpoints; cell viability via TBE and (pro)-inflammatory response with IL8. As shown in **Figure 1**, there was significant overlap with regards to the cytotoxicity of CuO ENM at the highest concentrations of 1 and 2  $\mu\text{g/ml}$  and both laboratories were in decisive agreement regarding the lack of cytotoxic response induced by 24-hour exposure to TiO<sub>2</sub> ENM. This data was then followed up by quantification of a (pro)-inflammatory response with the chemokine IL8. Both laboratories observed no significant induction of this chemokine at any test concentration for both TiO<sub>2</sub> and CuO ENMs, however a significant increase was observed across both laboratories when the spheroids were exposed to LPS. Therefore, it can be concluded that both laboratories, whilst following the PATROLS protocol for acute ENM exposures to HepG2 spheroids cultured via the hanging drop method, produced a harmonised data set.

### Advanced Lung Models

#### VitroCell Deposition

Despite the large experience of laboratory 1 and laboratory 2 in using VitroCell cloud devices, some differences have been recorded between the two institutes in terms of particle efficiency deposition, testifying that there's still need of improvement on this aspect. NC contribution (laboratory 2) was unexpectedly high (even after having applied the troubleshooting recommendations in case of high contribution from the vehicle, reported in

PATROLS SOP) while TiO<sub>2</sub> and CuO ENMs deposition values were close to the targeted dose of 1000 ng/cm<sup>2</sup>, as also achieved at laboratory 1 (**Figure 3**).

### Endpoint data

No reduction in cell viability (estimated via Alamar Blue assay) was observed after exposure to TiO<sub>2</sub> ENM. Different responses have been observed in laboratory 1 and 2 when CuO ENM were administered. Significant reduction of the metabolic activity (around 50%) was assessed in laboratory 1, while a not significant increase in metabolic activity was observed in laboratory 2. Considering the high contribution of vehicle (1% isotonic NaCl) to the deposition measured in laboratory 2, is not possible to exclude that during the exposure to CuO ENM the amount of ENMs effectively delivered was smaller than 1000 ng/cm<sup>2</sup>, thus not able to induce any significant reduction of the cell viability. The 3D models were responsive to Triton X-100 used as positive control for the cell viability assessment (1% final concentration).

To verify if any potential interference between the ENMs and the reagent of test (Alamar Blue working solution) could explain the differences observed, a fit-for-purpose experiment was performed by incubating each ENM with cell culture medium (CCM) or Alamar Blue solution (final concentration 400mM) and the Fluorescence Intensity of these suspensions was then measured by using the same settings applied for the biological samples.

Despite the differences observed by the two labs on the cell viability results, the data related to the quantification of IL8 after exposure to the ENMs are quite consistent. At the concentrations applied, both the ENMs didn't induce a significant release of IL8 in the medium. The 3D models were responsive to LPS (1 mg/ml) used as positive control for IL8 quantification through ELISA.

### HepaRG Data

Concerning the assays performed on 2D and 3D HepaRG cells, the results showed that TiO<sub>2</sub> ENM was non-cytotoxic and non-genotoxic in both models, although a small increase in the % tail DNA was noticed in the 3D model at 100 µg/ml. The two ZnO ENM induced a concentration dependent increase in cytotoxicity that was more pronounced in the 2D than in the 3D model. While the aqueous suspension of ZnO ENM displayed genotoxic effects mainly at cytotoxic concentrations, NM110 showed genotoxicity also at non-cytotoxic concentrations.

No major difference could be observed in the comet assay in the absence or in the presence of the Fpg enzyme, except for NM110 in the 2D model. Interestingly, the lower cytotoxicity in the 3D model enabled the detection of some genotoxicity at non-cytotoxic concentrations such as 25µg/ml for aq. ZnO or 25 and 50 µg/mL for NM110. By contrast, in the 2D model, cytotoxicity hindered the detection of formal genotoxicity, although some genotoxicity was detected for NM110 at 25 µg/ml. It must be outlined that, in the present study, the concentration regimen per cell is 35 times higher in the 3D model than in the 2D model but the exposure of spheroids to ENMs may not be give homogenous exposure of cells compared to the 2D system.





[www.riskgone.eu](http://www.riskgone.eu) | [riskgone@nilu.no](mailto:riskgone@nilu.no)

SWANSEA, 31 10 2022

*The publication reflects only the author's view and the European Commission is not responsible for any use that may be made of the information it contains.*



This project has received funding from the European Union's Horizon 2020 research and innovation programme under grant agreement No 814425.

- FERNÁNDEZ-CRUZ, M. L., HERNÁNDEZ-MORENO, D., CATALÁN, J., CROSS, R. K., STOCKMANN-JUVALA, H., CABELLOS, J., LOPES, V. R., MATZKE, M., FERRAZ, N., IZQUIERDO, J. J., NAVAS, J. M., PARK, M., SVENDSEN, C. & JANER, G. 2018. Quality evaluation of human and environmental toxicity studies performed with nanomaterials-the GUIDEnano approach. *Environmental Science: Nano*, 5, 381-397.
- LLEWELLYN, S. V., CONWAY, G. E., SHAH, U. K., EVANS, S. J., JENKINS, G. J. S., CLIFT, M. J. D. & DOAK, S. H. 2020. Advanced 3D Liver Models for In vitro Genotoxicity Testing Following Long-Term Nanomaterial Exposure. *J Vis Exp*.
- LLEWELLYN, S. V., KERMANIZADEH, A., UDE, V., JACOBSEN, N. R., CONWAY, G. E., SHAH, U. K., NIEMEIJER, M., MONÉ, M. J., VAN DE WATER, B., ROY, S., MORITZ, W., STONE, V., JENKINS, G. J. S. & DOAK, S. H. 2022. Assessing the transferability and reproducibility of 3D in vitro liver models from primary human multi-cellular microtissues to cell-line based HepG2 spheroids. *Toxicol In Vitro*, 85, 105473.

